Journal of Nuclear Materials 615 (2025) 156003

Contents lists available at ScienceDirect

Journal of Nuclear Materials

journal homepage: www.elsevier.com/locate/jnucmat

Physical interpretation of different experimental dependencies of the hydride reorientation stress threshold on the hydrogen content in Zircaloy-2, -4

Mikhail Kolesnik *, Juri Stuckert

Institute for Applied Materials – Applied Materials Physics (IAM-AWP), Karlsruhe Institute of Technology, Karlsruhe, Germany

ARTICLE INFO

Keywords:
Hydride embrittlement
Zirconium alloys
Dry storage
Reorientation of hydrides

ABSTRACT

The experimental dependences of the hydride reorientation stress threshold on the hydrogen concentration in zirconium alloys presented in various publications shows a significant divergence. This discrepancy may be due to different physical interpretations of the stress threshold: through minimal absolute amount of hydrogen (few ppm) or relative (few percent) amount of reoriented hydrides. This assumption was supported by simulations with the physically-based numerical tool. The paper proposes the concept of a "representative" stress threshold, defined by the relative amount of hydrogen in reoriented hydrides. The "representative" threshold characterizes the susceptibility of dissolved hydrogen to precipitate as radially oriented hydrides under external stresses.

1. Introduction

Hydride embrittlement of zirconium fuel rod cladding is one of the mechanisms limiting the handling and long-term dry storage regimes of spent nuclear fuel [1,2]. The degree of hydride embrittlement is largely determined by the morphology of the hydride network, as hydrides are able to provide the pathways for crack growth with low fracture energies [3]. The hydride morphology, in turn, can change during thermomechanical cycling when vacuum or gas drying of the cask with spent fuel assemblies is performed prior to transport or dry storage.

Hydrogen accumulated in fuel rod cladding during operation is almost completely in the hydride phase during storage in the fuel pool at low temperatures around 30 – 50 °C. The morphology of the hydrides after operation and cooling can be approximated as plates elongated in the circumferential direction of the cladding. If fuel assemblies are subjected to vacuum or gas drying, their temperature may increase due to decay heat generation and reach about 400 °C (the same temperature can be also reached at the beginning of dry storage), resulting in partial or complete dissolution of hydrides, depending on the total hydrogen content in the cladding and the maximum temperature. Undissolved hydrides retain their circumferential orientation, while hydrogen in solid solution can reprecipitate in the radial direction during subsequent cooling, depending on the external stresses generated by the internal gas pressure under the cladding. This process is known as hydride reorientation. Radial hydrides can increase the degree of hydride embrittlement and cause the ductile to brittle transition of the fracture mode if they are able to provide the almost continuous path for a brittle crack through the cladding. To avoid critical embrittlement during transport and storage, the thermomechanical regimes should minimize the radial hydride fraction (RHF).

The dependence of RHF on external stresses can be approximated as a threshold function: RHF has a very weak dependence on stresses below the threshold stress and grows with stresses at higher stresses [4,5]. At very high stresses all hydrides can precipitate in the radial direction, which marks the “high stress threshold”, or $\sigma_{th,100\ \%}$ (opposite to the “low stress threshold” where reorientation starts, $\sigma_{th,0\ \%}$) [6,7].

The concept of stress threshold has been widely used to estimate the reorientation tendency of hydrides in thermomechanical cycles [8–13] and is applied in a number of numerical models developed to predict RHF during dry storage [7,14,15]. This paper focuses on issues related to the physical interpretation of the stress threshold and its experimental dependencies, which have not yet been discussed.

2. The problem statement

The problem statement includes three separate issues, summarized in Table 1 and described in more detail below.

---

* Corresponding author.
E-mail address: mikhail.kolesnik@kit.edu (M. Kolesnik).

https://doi.org/10.1016/j.jnucmat.2025.156003
Received 5 May 2025; Received in revised form 18 June 2025; Accepted 23 June 2025

Table 1
A problem statement and the various interpretations of stress thresholds considered in the paper.

Issues	
1	discrepancy in the experimental dependence of the threshold on hydrogen concentration (at concentrations of hydrogen above the solubility limit)
2	an unclear physical interpretation of the experimental correlation for threshold (at hydrogen concentrations below the solubility limit)
3	an approach to experimental correlations of low and high thresholds in the limit of very low hydrogen concentrations
Interpretations of the low stress threshold	
1	stresses, at which 5 ppm of the hydrogen is present in radial hydrides
2	stresses, at which 5 % of the hydrogen in hydrides is present in radial hydrides
3	stresses, at which 5 % of the reprecipitated hydrogen (dissolved and precipitated during the thermomechanical cycle) is present in radial hydrides

2.1. Issue 1. Unexplained discrepancy in experimental data (for concentrations above the solubility limit in the thermocycle)

The first issue follows from the comparison of experimental data [6–9] where the hydride reorientation threshold has been measured under similar conditions for different hydrogen concentrations above the solubility limit in the thermomechanical cycle. As can be seen from Fig. 1, there are significant differences both in absolute values and in the type of dependence after thermomechanical cycles:

- in [6] and [7] the experimental stress threshold is almost constant above the solubility limit and is around 60 MPa for 350 °C, or 30 – 35 MPa for 400 °C;
- in [8] and [9] the stress threshold has a strong dependence on hydrogen concentration and growth from ≈ 60 – 70 MPa at the solubility limit to around 160 MPa at 600 ppm and 350 °C, or 140 MPa at 600 ppm and 400 °C.

The conditions of experiments [6,8,9] are very similar: in each case, the stress threshold was measured as a result of a thermomechanical cycle with a maximum temperature of 350 or 400 °C and a constant load during cooling. The cooling rates were in the range 0.4 – 0.7 °C/min in all experiments [6,8,9].

The loading schemes in the experiments are different, but the general concept is the same. The experimental methods are based on compression of C-shaped specimens in [6] and tension of cladding tube segments in [8] and [9]. In both methods, the local morphology of the hydrides is compared with the local stress state calculated by FEM, and therefore the difference in loading schemes should not affect the experimental results. The authors of [6] also described these two experimental methods as "comparable".

Experiments on Zircaloy-4 [9] and Zircaloy-2 with the inner liner removed [8] showed similar results, while data [6] and [7] for Zircaloy-4 differed from both [8] and [9] experimental results. There is no obvious physical mechanism that could cause different hydride reorientation in Zircaloy-2 and Zircaloy-4, as they have similar chemical composition, mechanical properties and microstructure, and the hydride reorientation behavior of these alloys is considered here to be similar.

In conclusion, different alloys and loading schemes cannot explain the difference in experimental results shown in Fig. 1. This paper proposes an alternative explanation in Section 3.

2.2. Issue 2. Unclear physical interpretation of the engineering correlations (for concentrations below the solubility limit in the thermomechanical cycle)

Authors of [6] suggested the following engineering correlations for stress threshold $\sigma_{th,0\ \%}$ in [MPa] on hydrogen concentrations:

$$\sigma_{th,0\%} = 0.02\cdot C_{tot} + 186.9 - 0.3862\cdot \min(T_{\max}, T_{ssd}) \qquad (1)$$

C_{tot} – total hydrogen concentration [ppm], $T_{\max}$ – maximal temperature of the thermocycle [°C], T_{ssd} – temperature of the complete dissolution of hydrides [°C]. Correlation (1) for different temperatures and experimental points [6,7] is shown in Fig. 2.

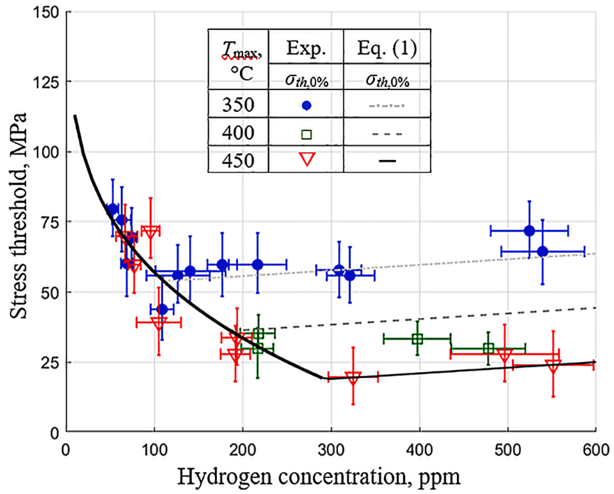

Fig. 2. Comparison of experimental data [6,7] and correlation Eq. (1); black line – the common part of the correlations for different temperatures.

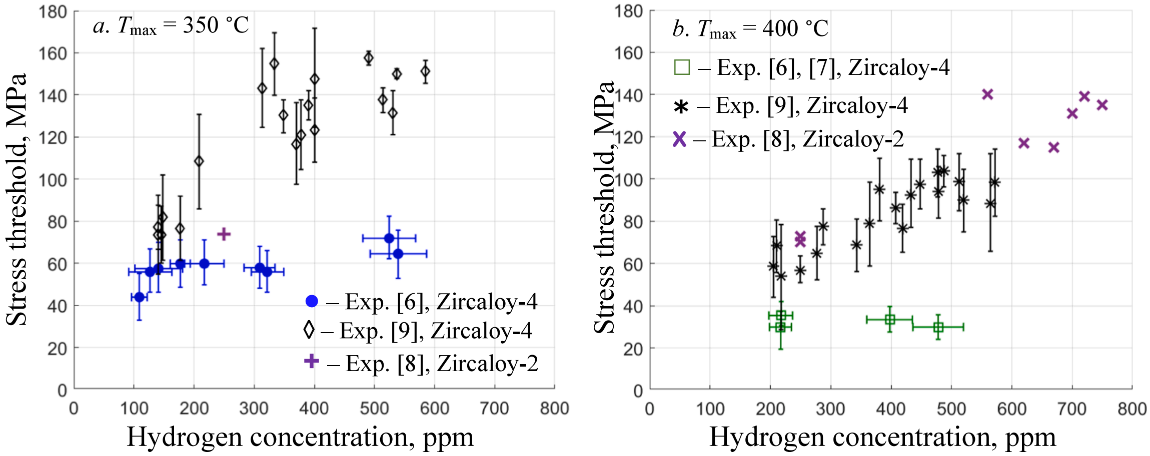

Fig. 1. Different dependencies of hydride reorientation thresholds established in experiments [6,7] and [8,9]; for concentrations above the solubility limit in the thermocycle, which are ≈ 110 ppm for $T_{\max}$ = 350 °C and ≈ 200 ppm for $T_{\max}$ = 400 °C.

As can be seen from Fig. 2, the correlation Eq. (1) has a breaking point at a concentration equal to the solubility limit at the maximum temperature of the thermomechanical cycle. At lower concentrations, the threshold increases significantly with decreasing hydrogen concentration (from ≈ 20 MPa at 300 ppm to ≈80 MPa at 50 ppm). The physical mechanism of this dependence was not explained in [6] and remains unclear. Moreover, this dependence may contradict to theoretical models based on Ells' approach [16] that assumes the dependence of the radial hydride fraction F_r on stress divided by temperature (σ/T). As the hydride precipitation temperature decreases with decreasing hydrogen concentration, the stress threshold $\sigma_{th,0\ \%}$ should also decrease proportionally to temperature to achieve the same radial hydride fraction $F_{r,\mathrm{min}}(\sigma_{th,0\ \%}/T)$. This contradicts the correlation Eq. (1) and experimental points on Fig. 2. Section 3 proposes an assumption that brings together the physical model and the experimental data.

2.3. Issue 3. Unclear physical interpretation of the correlations limit at very low concentrations

The stress threshold $\sigma_{th,100\ \%}$ characterizes the stress above which almost all hydrides precipitate in the radial direction. In [6], the following engineering correlation was proposed for the dependence of $\sigma_{th,100\ \%}$ in [MPa] on the hydrogen concentration:

$$\sigma_{th,100\%} = 110 + 65(1 - \exp(-C_{tot}/65)) \pm 20 \qquad (2)$$

The correlations Eqs. (1) and (2) as well as the experimental data [6] used for their development are compared in Fig. 3. As can be seen from Fig. 3, both correlations for $\sigma_{th,0\ \%}$ and $\sigma_{th,100\ \%}$ tend to overlap at low concentrations and intersect at about 5 ppm (beyond the range of experimental conditions). The physical interpretation is that the radial hydride fraction F_r can only be 0 % or 100 % at such conditions but not in the range $0\,\% < F_r < 100\,\%$. This feature of the engineering correlation Eqs. (1) and (2), as well as the reduction of stress range of mixed hydride orientation $\Delta\sigma_{th} = \sigma_{th,100\ \%} - \sigma_{th,0\ \%}$ from $\Delta\sigma_{th} \approx 150$ MPa at 200 ppm to $\Delta\sigma_{th} \approx 50$ MPa at 70 ppm requires an explanation of the physical mechanism.

3. The proposed solution

3.1. General solution framework

The proposed solution to the above issues is based on the assumption that the hydride reorientation thresholds in different experimental methods may have a difference in physical interpretations, formulated in Table 1.

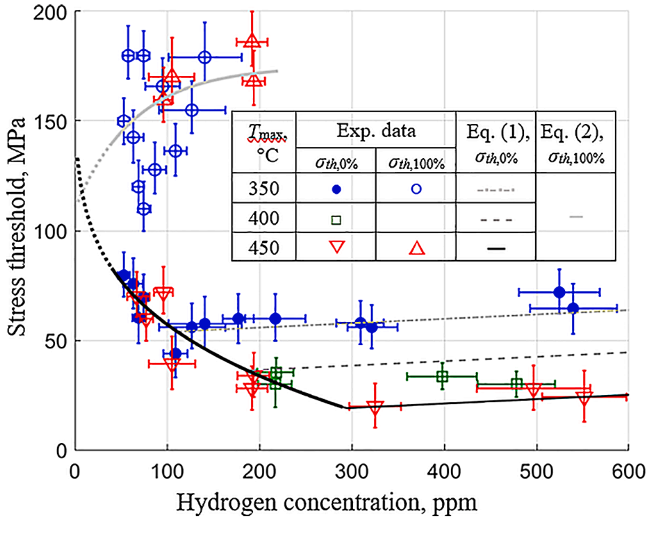

Fig. 3. Stress thresholds $\sigma_{th,0\ \%}$ and $\sigma_{th,100\ \%}$ in [6,7]; dotted lines – extrapolation beyond the range of experimental data showing almost equivalence of the lower and upper thresholds at low concentrations.

The stress threshold for hydride reorientation is defined in [6] as the minimum local stress within the compressed C-shaped sample, at which a single radially oriented hydride can be detected (follows from Fig. 6 in [6] and Fig. 9 in [17], where the same method is described). Even a single experimentally detectable radial hydride requires a certain amount of hydrogen. Therefore, the stress threshold in [6] can be defined as the stress at which a minimum absolute amount of hydrogen (e.g. a few ppm) precipitates as radial hydrides.

The stress threshold for hydride reorientation in [9] has a different interpretation. Following the method previously used in [18], the stress threshold was defined as stresses at which the relative fraction of radial hydrides exceeds the as-hydrided value (without external stresses) by 5 %. Contrary to the method used in [6], the radial hydrides can be present at local stresses below the stress threshold, as can be seen from Fig. 5 in [9] and Figs. 5 and 6 in [18].

The authors of [8] define the stress threshold as a statistical mean of minimum local stresses at which radial hydrides can be detected. This method assumes that radial hydrides can be present at stresses below the threshold, as can be seen in Fig. 8 in [8]. Therefore, the interpretation of the stress threshold is slightly different from that in [6] and it is assumed in this paper that the stress threshold in [6] may represent the stress at which the relative proportion of hydrides exceeds a minimum value (e.g. a few percent), as in [9].

Further analysis is based on the assumption, that in hydride reorientation tests with small samples (C-shape tests [6] and ring tests [8,9]) two implicit interpretations of the stress threshold may exist: as stresses required to reorient a minimum absolute (e.g. a few ppm) or relative (e.g. a few percent) amounts of hydrides. It is expected that at high hydrogen concentrations and dense hydride networks the difference in interpretation will be clear, allowing the local radial hydride fraction to be estimated. At low concentrations (especially below 100 ppm), it may be difficult to define the local radial hydride fraction due to the small number of hydrides in the narrow isostress layer of ≈10 μm wide. This may lead to a blurring of the difference between two interpretations in favor of the threshold defined by absolute values at low hydrogen concentrations. Note, that the feature of different interpretations of stress thresholds is relevant for experiments with small samples and high stress gradients, which can be up to 500 – 1000 MPa/mm (based on Fig. 7 in [8] and Fig. 3 in [9]). For experiments with low stress gradients or with homogeneous stresses, e.g. gas-filled tubes [18,19] or loaded planes [4], the hydride reorientation threshold is defined by a minimum relative fraction of reoriented hydrides (usually, ≈ 5 %).

3.2. Comparison of the experimental thresholds with simulations

The dependence of the stress threshold on the hydrogen concentration in both interpretations was calculated using a simulation tool based on Ells' approach [16] and kinetic models [20] and [21], which is described in Appendix. The temperature scenario used in the simulations was close to that used in the experiments [6,8] and [9]: linear heating from room temperature to T_{max} (350, 400 or 450 °C), holding at T_{max} for one hour and slow cooling in the presence of external stresses. The initial orientation of the hydrides was assumed to be 100 % circumferential.

The model has been used to simulate the reorientation curves, i.e. the dependence of the hydrogen concentration in the radial hydrides and radial hydride fraction on external stresses, under the conditions of the experiments [6,8] and [9]. The stress thresholds have then been estimated from these reorientation curves in two approximations: 1) as the stress, at which the hydrogen concentration in radial hydrides exceeds 5 ppm, and 2) as the stress at which the radial hydride fraction exceeds 5 %. The first is compared with experimental data [6,7] in Fig. 4; the second is compared with experimental data [8,9] in Fig. 5. The

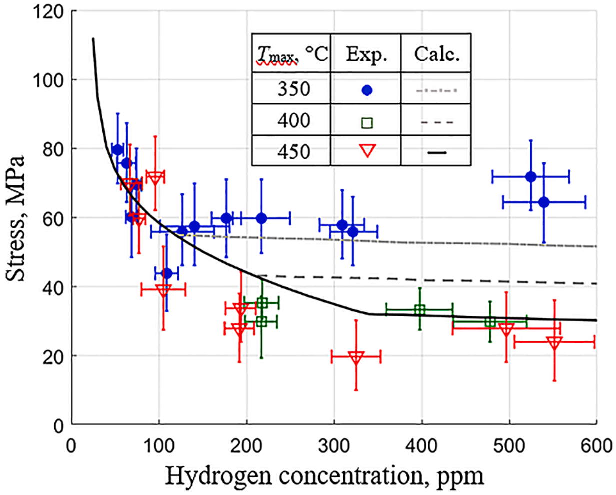

Fig. 4. The calculated stresses at which 5 ppm hydrogen precipitates as radially oriented hydrides compared to the experimental stress threshold $\sigma_{th,0\ \%}$ [6, 7] (Zircaloy-4).

calculated lines in Figs. 4 and 2 are similar, but their origin is different: the lines in Fig. 2 are engineering correlations, while the lines in Fig. 4 are the result of simulations with a model based on general physical assumptions.

Note, that the dash-dotted line in Figs. 4 and 5*a* and dashed line in Figs. 4 and 5*b* represent the same simulation results, but in different interpretations resulted in different dependencies of stress thresholds on hydrogen concentrations. The agreement between the simulation results and the experimental data is considered acceptable. Although the absolute values for some conditions may differ between experiment and simulation, the model correctly predicts the main features of the experimental dependencies. The stress threshold, defined by absolute values of the hydrogen concentration in radial hydrides, decreases rapidly with increasing hydrogen concentration for samples with complete dissolution of hydrides and remains almost constant for samples with incomplete dissolution, as the threshold in experiments [6,7] (Fig. 4). The threshold, defined by relative values of the radial hydride fraction, increases with hydrogen concentration for samples with incomplete dissolution of hydrides as the threshold in experiments [8,9] (Fig. 5). Therefore, the simulation has confirmed that the different interpretation of the stress threshold can explain the divergence between the experimental data shown in Fig. 1 thus solving the Issue 1 (Section 2.1).

4. Discussion

4.1. Physical interpretations of different experimental dependencies

The assumption of two different interpretations of stress thresholds in small-sample experiments reveals the physical interpretations of different experimental dependencies.

The threshold defined by absolute values (e.g. the hydrogen concentration in radial hydrides of 5 ppm) decreases with increasing hydrogen concentration for samples with complete hydride dissolution (Fig. 4, low concentrations). This is due to the reduction in the relative fraction of 5 ppm used to define the threshold: 5 ppm is 10 % of 50 ppm but only 2.5 % of 200 ppm. The stresses required to reorient 10 % of the hydrides should be much higher than those required to reorient 2.5 % of the hydrides. Therefore, the threshold defined in this way is much higher for 50 ppm than for 200 ppm, as can be seen from Fig. 6*a*, which can explain part of the engineering correlation Eq. (1) for $T_{\max} > T_{ssd}$ and solve Issue 2 (Section 2.2).

At high hydrogen concentrations and incomplete dissolution of hydrides, the stress threshold defined by the absolute values is almost constant for a constant maximum temperature (Fig. 4, high concentrations). This is because the same amount of hydrogen, corresponding to the solubility limit, dissolves and then reprecipitates under the same conditions, irrespective of the total hydrogen concentration. The reorientation curves in absolute values are almost the same and give the same threshold, as can be seen from Fig. 6*b*

The threshold, determined by relative values of the radial hydride fraction, increases with increasing hydrogen concentration (Fig. 5*a* and 5*b*). For samples with complete hydride dissolution, it is explained by the dependence of the radial hydride fraction on the temperature $F_r(\sigma/T)$ in models based on the Ells' approach [16]. The effect of hydride precipitation temperature on the degree of reorientation in relative terms can be seen in Fig. 7*a*. A further increase in the threshold for samples with incomplete hydride dissolution is due to the greater amount of hydrogen that must be reorientated as the hydrogen concentration increases. The 5 % at 200 ppm is 10 ppm, while at 800 ppm it is 40 ppm, while the concentration of the hydrogen dissolved at maximum temperature is the same for both samples (around 200 ppm for $T_{\max} = 400$ °C). The threshold defined in this way is therefore higher for 800 ppm than for 200 ppm because the stresses required to reorient 10 of 200 ppm in the 200 ppm samples are lower than the stresses required to reorient 40 of 200 ppm (the solubility limit at 400 °C) in the 800 ppm samples, as can be seen from Fig. 7*b*

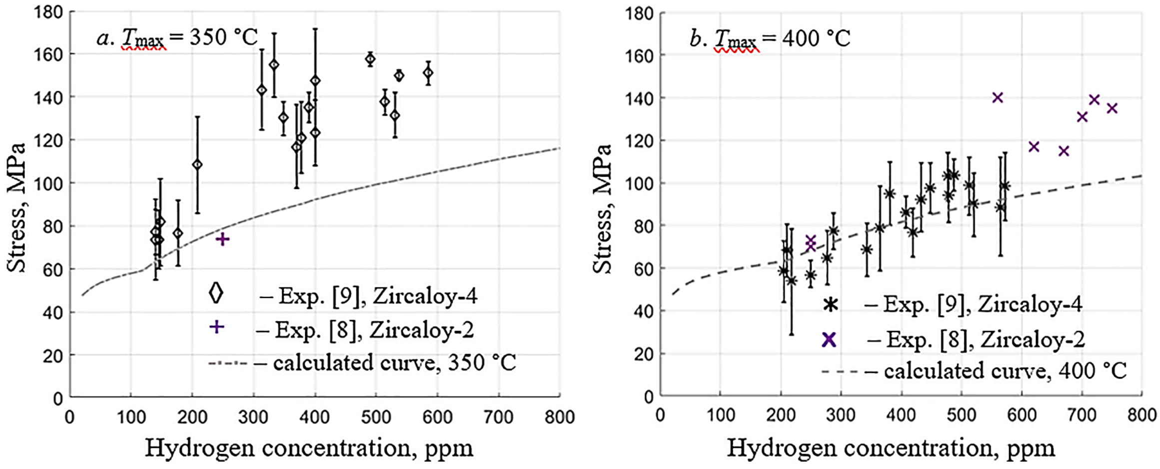

Fig. 5. The calculated stresses, at which 5 % of hydrogen precipitates as radially oriented hydrides compared to the experimental stress threshold [8,9].

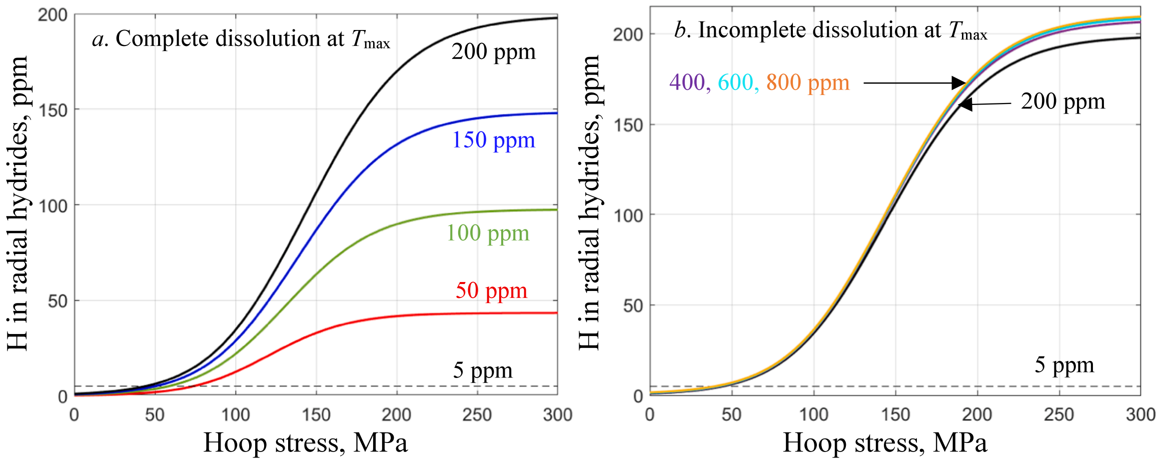

Fig. 6. Calculated reorientation curves for different total hydrogen concentrations in case of using absolute threshold values; T_{max} = 400 °C.

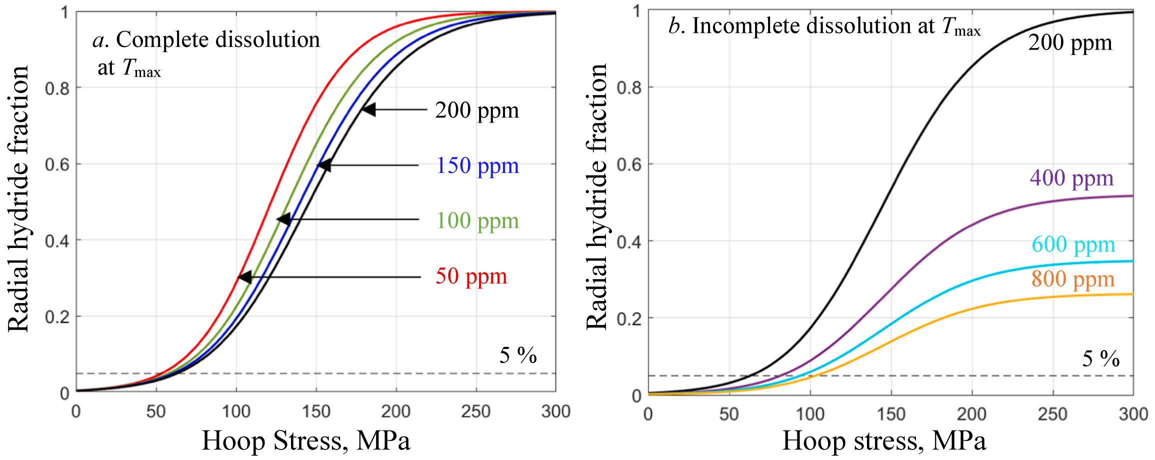

Fig. 7. Calculated reorientation curves in relative values; T_{max} = 400 °C.

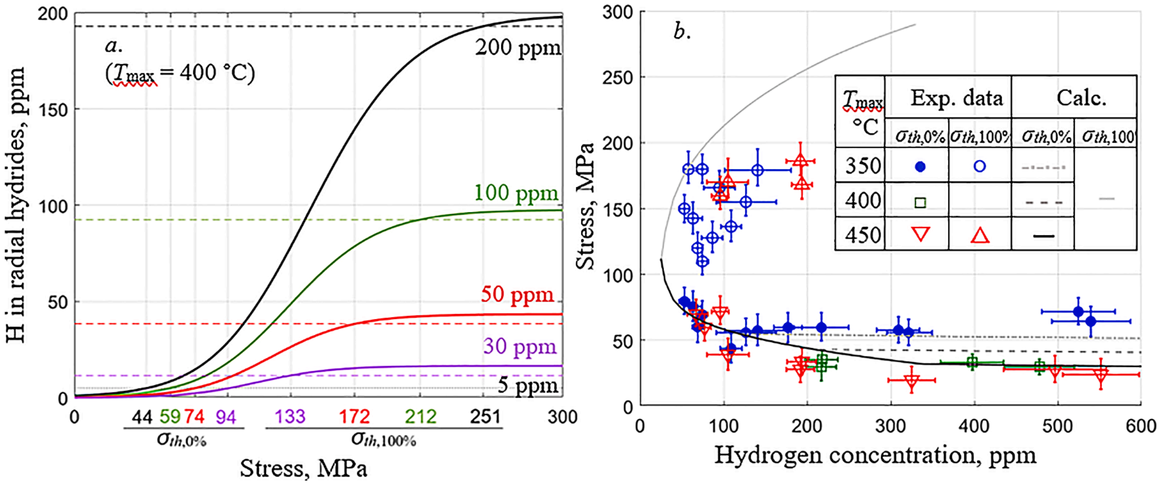

Fig. 8. Equivalence of calculated thresholds $\sigma_{th,0\ \%}$ and $\sigma_{th,100\ \%}$ defined through absolute values at low concentrations; *a* – reorientation curves and their stress thresholds for different hydrogen concentrations; $\sigma_{th,0\ \%}$ is defined as the stress at which 5 ppm is present in the radial hydrides (the intersection of the dotted line with the curves), $\sigma_{th,100\ \%}$ is defined as the stress at which 5 ppm is present in the circumferential hydrides (the intersection of the dashed line with the curve); *b* – calculated low and high stress thresholds compared with experimental data [6,7].

4.2. Physical interpretation of equivalence thresholds $\sigma_{th,0\ \%} = \sigma_{th,100\ \%}$ in correlations [6] at very low concentrations

It was assumed that the experimental data [6,7], which were the basis for the correlations Eqs. (1) and (2), represent the threshold determined by the minimum absolute amount of reoriented hydrides. This assumption allowed to simulate the experimental result for the low stress threshold $\sigma_{th,0\ \%}$ with acceptable agreement (Fig. 4). The high stress threshold $\sigma_{th,100\ \%}$ can be determined from calculated reorientation curves in a similar way to the stresses at which only 5 ppm of hydrogen precipitates as circumferential hydrides. The procedure for estimating both thresholds is shown in Fig. 8*a* for four different hydrogen contents and $T_{\max} = 400$ °C and gives the qualitative agreement with the experimental data, as can be seen in Fig. 8*b* Both thresholds move towards each other as the total hydrogen concentration decreases (Fig. 8*a*). The coincidence of thresholds occurs when about 10 ppm precipitates in the hydride phase: 5 ppm as radial hydrides and 5 ppm as circumferential, i.e. low and high thresholds are formally equivalent. This interpretation can explain the physical basis of the correlations Eqs. (1), (2) and their intersection in the limit of very low concentrations, which solves Issue 3 (Section 2.3).

4.3. The “representative” stress threshold

Defining the stress threshold in absolute or relative terms can lead to different values and different types of dependence on hydrogen concentration, as can be seen from Figs. 4 and 5. This raises the question of which interpretation is more representative as a value characterizing the susceptibility of hydrides to reorientation under external stresses.

As discussed in Section 3.1, the dependence of the threshold defined through absolute values of the hydrogen content at low concentrations can be interpreted, as meaning that the lower fraction of hydrides requires the lower stress to be reoriented (Figs. 4 and 6*a*). This obvious fact does not reflect the susceptibility of hydrides to reorientation at different hydrogen concentrations.

A similar issue arises with the threshold defined by relative values at high concentrations. Its dependence on hydrogen content can be interpreted as the higher the concentration of undissolved hydrogen, the higher the fraction of dissolved hydrogen that should be reoriented, which requires higher stresses. Thus, the increase in stress threshold at high concentrations observed in Fig. 5 reflects the increasing role of undissolved hydrides, which dilute the fraction of reoriented hydrides. This mechanism also does not reflect the susceptibility of dissolved and reprecipitated hydrides to reorientation.

The stress threshold, which represents the susceptibility of dissolved hydrogen to precipitate as radially oriented hydrides, can be determined as the stresses required to precipitate a certain fraction of dissolved hydrogen (0.05, according to the most popular value) into reoriented hydrides. This condition is referred to as the threshold interpretation 3 in Table 1 and is equivalent to the renormalized hydride reorientation curve:

$$\frac{C_r(\sigma_{th})}{\min(C_{tot}, C_{ssd}(T_{\max}))} \simeq \frac{F_r(\sigma_{th}) - F_r(\sigma \to 0)}{F_r(\sigma \to \infty) - F_r(\sigma \to 0)} = 0.05 \tag{3}$$

The calculated dependence of stress threshold defined by Eq. (3) on hydrogen concentrations is shown on Fig. 9. The interpretation of the threshold suggested in Eq. (3) differs from the two used above and is considered here to be the most "representative" in regard to the susceptibility to reorientation of dissolved and reprecipitated hydrogen during the thermomechanical cycle.

All calculated lines in Figs. 4, 5 and 9 represent the same simulation results calculated with the same model parameters. The only difference is the interpretation of the stress threshold estimated by the reorientation curve in absolute, relative, or renormalized relative values. Different physical interpretations lead to different, and sometimes opposite, dependencies of the threshold on the hydrogen concentration.

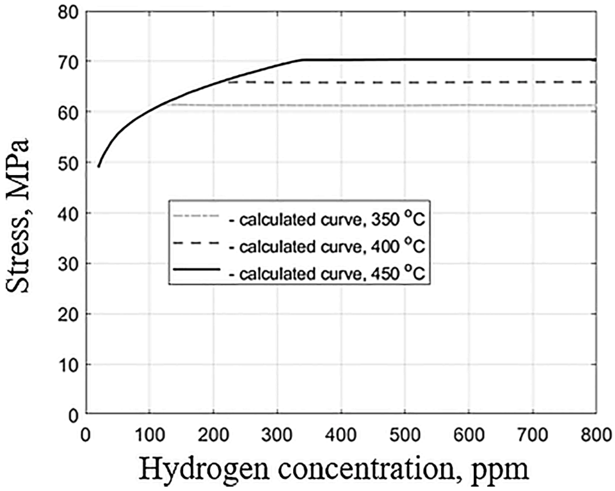

Fig. 9. The calculated “representative” threshold, defined by Eq. (3).

4.4. Important aspects outside the scope of the study

An important feature of the experiments considered here is the loading scheme in ring tests (ring tension or compression), which produces high stress gradients of up to 500–1000 MPa/mm throughout the thickness of the ring (based on Fig. 7 in [8] and Fig. 3 in [9]), and leads to the redistribution of hydrogen in a solid solution at high test temperatures. In [9], the radial stress gradient in ring tests was identified as the cause of the threshold’s dependence on hydrogen content at low concentrations, providing an alternative explanation for Issue 2. In the current investigation, we have neglected the stress gradient factor, but have not excluded it. Indeed, when cooling a sample with heterogeneous hydrogen concentration, hydrides will precipitate in different zones at different temperatures. The first precipitated hydrides are expected to be radial, as the highest hydrogen concentration will be found in the zone experiencing the greatest tensile stress. As they grow during cooling, these radial hydrides will penetrate neighboring radial zones with lower local stresses. This means that the hydrides formed in one radial zone can influence the morphology of neighboring zones. This in turn may affect the measured threshold, particularly at low hydrogen concentrations.

Another important point to note is that if stress threshold is applied as the only parameter, it is unable to predict the risk of fracture or the hydride-induced ductile-to-brittle transition of fracture mode in zirconium alloys. While it indicates whether the noticeable part of the hydrides is reoriented after the thermomechanical cycle, it provides no information about the length of the hydrides, the distance between them, or the continuity of the hydride network. These factors largely determine crack nucleation and growth [3]. The necessary conditions for the ductile-to-brittle transition in terms of hydrogen morphology can be formulated as percolation of the hydride network (i.e. the hydride network must be able to provide an almost continuous short path for a brittle crack through the sample) [3].

The extremely high hydrogen concentrations (e.g. in the rim layer or hydride blister) also limit the simplified approach based on the orientation of the hydrides. If the hydride network fills all the grain boundaries or forms a solid bulk hydride, the material becomes brittle [23] and the radial hydride fraction loses its meaning. Another limiting case is duplex cladding with a liner. If sufficient time is spent at a high temperature, the liner and the interface will accumulate almost all the hydrogen from the cladding, leaving the substrate almost free of hydrides after cooling [24,25]. In such conditions, the degree of reorientation of the hydrides in duplex cladding is also not the main factor that characterizes fracture behavior.

5. Conclusion

A generalized approach to the different interpretations of the reorientation stress threshold (by the absolute and relative amount of hydrogen in reoriented hydrides) made it possible to eliminate the apparent discrepancy between experimental data and to provide a physical interpretation of various experimental dependencies on hydrogen concentration. Following this approach, the kinetic model based on Ells' approach [16] and kinetic models [20] and [21] is able to simulate both types of experimental dependencies discussed in this paper.

The application of the stress threshold as a universal parameter to simulate hydride reorientation after thermomechanical testing may be an oversimplified approach. The simulation should consider the fraction of dissolved (able to reorient) and undissolved (unable to reorient) hydrogen at the maximum temperature of the thermocycle. The paper proposes the definition of the "representative" stress threshold, defined by the amount of hydrogen converted to radial hydrides relative to the total amount of dissolved hydrogen. Such a threshold characterizes the susceptibility of dissolved hydrogen to precipitate as radially oriented hydrides under external stresses.

CRediT authorship contribution statement

Mikhail Kolesnik: Writing – original draft, Formal analysis, Data curation, Conceptualization. **Juri Stuckert:** Writing – review & editing, Supervision, Project administration.

Declaration of competing interest

The authors declare that they have no known competing financial interests or personal relationships that could have appeared to influence the work reported in this paper.

Appendix. Description of the model used for simulations

A kinetic hydride reorientation model used for simulations in this paper is based on Ells' approach [16] and the models developed in [20] and [21]. Mathematically, the model is the numerical solution of the ODE system with two independent model variables: concentration of hydrogen in solid solution C_s and fraction of radially-oriented hydrides θ.

The dissolution of hydrides occurs when the hydrogen concentration in the solid solution C_s is below the solubility for dissolution C_{ssd} ($C_s < C_{ssd}$) and temperature T is below the temperature of complete hydride solubility T_{ssd} ($T < T_{ssd}$) and is described by:

$$\begin{cases} \dfrac{\mathrm{d}C_s}{\mathrm{d}t} = \dfrac{C_{ssd} - C_s}{\tau_0} \\ \dfrac{\mathrm{d}\theta}{\mathrm{d}t} = 0 \end{cases} \tag{4}$$

τ_0 – diffusional relaxation time. It can be estimated as $\tau_0 \approx l^2/(\alpha^2 D_\mathrm{H})$ [20], where $\alpha \approx 0.5$ –geometry factor, D_H –hydrogen diffusional coefficient, l –inter-precipitate distance; according to [20] $l \approx 6.7 \times 10^3 \times h/C_\mathrm{tot}$, where $h \approx 0.5$ μm –hydride thickness and C_tot –total hydrogen concentration in the sample in [wppm].

The precipitation of hydrides occurs when the hydrogen concentration in the solid solution C_s exceeds the solubility for precipitation C_{ssp} ($C_s > C_{ssp}$) and is described as:

$$\begin{cases} \dfrac{\mathrm{d}C_s}{\mathrm{d}t} = \dfrac{C_{ssp} - C_s}{\tau_0} \\ \dfrac{\mathrm{d}\theta}{\mathrm{d}t} = -\dfrac{f_r - \theta}{C_{tot} - C_s} \cdot \dfrac{\mathrm{d}C_s}{\mathrm{d}t} \end{cases} \tag{5}$$

f_r –instantaneous fraction of radially-oriented hydrides, which is a function of instantaneous stress σ and temperature T:

$$f_r = \frac{1}{1 + f_0 \cdot \exp(-\sigma \cdot \Delta\Omega / kT)} \tag{6}$$

where f_0 and $\Delta\Omega$ are model parameters, characterizing the susceptibility of hydride to reorientation.

For C_s values between C_{ssd} and C_{ssp} ($C_{ssd} \le C_s \le C_{ssp}$) neither precipitation nor dissolutions of hydrides is assumed (solubility hysteresis): $\mathrm{d}C_s/\mathrm{d}t = 0$ and $\mathrm{d}\theta/\mathrm{d}t = 0$.

The values of model parameters used in simulations are summarized in the Table A1.

Table A1
The values of the model parameters.

Parameter	Value	Unit	Reference
f_0	200	–	best estimation
$\Delta\Omega$	2.64×10^{-28}	m^3	
C_{ssd}	$2.255 \times 10^5 \times \exp(-39{,}101/RT)$	ppm	[22]
C_{ssp}	$8.612 \times 10^5 \times \exp(-30{,}583/RT)$	ppm	[22]
D_H	$1.17 \times 10^{-7} \times \exp(-4041.2/T)$	m^2/s	[20]

Data availability

No data was used for the research described in the article.

References

[1] M.P. Puls, The Effect of Hydrogen and Hydrides on the Integrity of Zirconium Alloy Components, Springer-Verlag, London, 2012, https://doi.org/10.1007/978-1-4471-4195-2.

[2] A.T. Motta, et al., Hydrogen in zirconium alloys: a review, J. Nucl. Mater. 518 (2019) 440–460, https://doi.org/10.1016/j.jnucmat.2019.02.042.

[3] M. Kolesnik, Micro-mechanisms of the ductile-to-brittle transition in hydrogenated zirconium alloys: a review and a comparison analysis of experimental data and theoretical approaches, Eng. Fail. Anal. (2024) 108110, https://doi.org/10.1016/j.engfailanal.2024.108110.

[4] D. Hardie, M.W. Shanahan, Stress reorientation of hydrides in zirconium-2.5 % niobium, J. Nucl. Mater. 55 (1975) 1–13, https://doi.org/10.1016/0022-3115(75)90132-4.

[5] J.B. Bai, N. Ji, D. Gilbon, C. Prioul, D. François, Hydride embrittlement in ZIRCALOY-4 plate: part II. interaction between the tensile stress and the hydride morphology, Metall. Mater. Trans. A 25 (1994) 1199–1208, https://doi.org/10.1007/BF02652294.

[6] J. Desquines, et al., Influence of temperature and hydrogen content on stress-induced radial hydride precipitation in Zircaloy-4 cladding, J. Nucl. Mater. 453 (2014) 131–150, https://doi.org/10.1016/j.jnucmat.2014.06.049.

[7] J. Desquines, C. Sartoris, M. Guémas, A. Gérard, Radial hydride precipitation in fuel cladding during back-end cooling transient under decreasing pressure, in: WRFPM 2023, 299, Springer, Singapore, 2024, https://doi.org/10.1007/978-981-99-7157-2_8.

[8] A.M. Alam, C. Hellwig, Cladding tube deformation test for stress reorientation of hydrides, J. ASTM Int. 5 (2008) 635–650, https://doi.org/10.1520/JAI101110.

[9] J.M. Lee, H.A. Kim, D.H. Kook, Y.S. Kim, A study on the effects of hydrogen content and peak temperature on threshold stress for hydride reorientation in Zircaloy-4 cladding, J. Nucl. Mater. 509 (2018) 285–294, https://doi.org/10.1016/j.jnucmat.2018.07.005.

[10] S. Valance, J. Bertsch, Hydrides reorientation investigation of high burn-up PWR fuel cladding, J. Nucl. Mater. 464 (2015) 371–381, https://doi.org/10.1016/j.jnucmat.2015.05.003.

[11] K. Colas, A. Motta, M.R. Daymond, J. Almer, Mechanisms of hydride reorientation in Zircaloy-4 studied in Situ, in: Zircon. Nucl. Ind. 17th Int. Symp., 2015, pp. 1107–1137, https://doi.org/10.1520/stp154320120168.

[12] Q. Auzoux, et al., Hydride reorientation and its impact on mechanical properties of high burn-up and unirradiated cold-worked stress-relieved Zircaloy-4 and ZirloTM fuel cladding, J. Nucl. Mater. 568 (2022) 15383, https://doi.org/10.1016/j.jnucmat.2022.153893.

[13] Y.J. Kim, D.H. Kook, T.H. Kim, J.S. Kim, Stress and temperature-dependent hydride reorientation of Zircaloy-4 cladding and its effect on the ductility degradation, J. Nucl. Sci. Technol. 52 (2014) 717–727, https://doi.org/10.1080/00223131.2014.978829.

[14] F. Feria, C. Aguado, L.E. Herranz, Extension of FRAPCON-xt to hydride radial reorientation in dry storage, Ann. Nucl. Energy 145 (2020) 107559, https://doi.org/10.1016/j.anucene.2020.107559.

[15] P. Konarski, C. Cozzo, G. Khvostov, H. Ferroukhi, Spent nuclear fuel in dry storage conditions – current trends in fuel performance modeling, J. Nucl. Mater. 555 (2021) 153138, https://doi.org/10.1016/j.jnucmat.2021.153138.

[16] C.E. Ells, The stress orientation of hydride in zirconium alloys, J. Nucl. Mater. 35 (1970) 306–315, https://doi.org/10.1016/0022-3115(70)90214-X.

[17] V. Busser, J. Desquines, C. Duriez, M.C. Baitto-Dubong, J.P. Mardon, Zircaloy-4 cladding hydride reorientation under RIng compression test conditions, in: Water Reactor Fuel Perfromance Meeting, 2009, pp. 292–299, https://doi.org/10.13140/2.1.2563.9363. Paper 2104.

[18] J.S. Kim, Y.J. Kim, D.H. Kook, Y.S. Kim, A study on hydride reorientation of Zircaloy-4 cladding tube under stress, J. Nucl. Mater. 456 (2015) 246–252, https://doi.org/10.1016/j.jnucmat.2014.09.032.

[19] H.C. Chu, S.K. Wu, R.C. Kuo, Hydride reorientation in Zircaloy-4 cladding, J. Nucl. Mater. 373 (2008) 319–327, https://doi.org/10.1016/j.jnucmat.2007.06.012.

[20] A.R. Massih, L.O. Jernkvist, Stress orientation of second-phase in alloys: hydrides in zirconium alloys, Comput. Mater. Sci. 46 (2009) 1091–1097, https://doi.org/10.1016/j.commatsci.2009.05.025.

[21] M. Kolesnik, T. Aliev, V. Likhanskii, Modeling of size, aspect ratio, and orientation of flattened precipittes in the context of Zr-H system under external stress, Comp. Mater. Sci. 189 (2021) 110260, https://doi.org/10.1016/j.commatsci.2020.110260.

[22] J.S. Kim, Y.S. Kim, Effect of thermal history on the terminal solid solubility of hydrogen in Zircaloy-4, Int. J. Hydrogen Energy 39 (2014) 16442–16449, https://doi.org/10.1016/j.ijhydene.2014.08.018.

[23] A. Pshenichnikov, J. Stuckert, M. Walter, Hydride precipitation, fracture and plasticity mechanisms in pure zirconium and zircaloy-4 at temperatures typical for the postulated loss-of-coolant accident, Nucl. Eng. Des. 301 (2016) 366–377, https://doi.org/10.1016/j.nucengdes.2016.03.024.

[24] Q. Auzoux, et al., Hydride reorientation and its impact on ambient temperature mechanical properties of high burn-up irradiated and unirradiated recrystallized Zircaloy-2 nuclear fuel cladding with an inner liner, J. Nucl. Mater. 494 (2017) 114–126, https://doi.org/10.1016/j.jnucmat.2017.07.022.

[25] A.-M. Alvarez, J. Stjärnsäter, J. Karlsson, A. Benen, P. Tejland, K.D. Johnson, R. Josek, Evaluation of the hydride reorientation behavior for Zircaloy-2 liner cladding with high hydrogen content during interim dry storage conditions, in: S. K. Yagnik, M. Preuss (Eds.), Zircon. Nucl. Ind. 20th Int. Symp., ASTM International, West Conshohocken, PA, 2023, pp. 673–694. http://doi.org/10.1520/STP164520220013.